

## Effect of Local Molecular Structure on the Chain-Length Dependence of the Electronic Properties of Thiophene-Based $\pi$ -Conjugated Systems

Pierre Frère,<sup>\*,†</sup> Jean-Manuel Raimundo,<sup>†</sup> Philippe Blanchard,<sup>†</sup> Jacques Delaunay,<sup>†</sup> Pascal Richomme,<sup>‡</sup> Jean-Louis Sauvajol,<sup>§</sup> Jesus Orduna,<sup>||</sup> Javier Garin,<sup>||</sup> and Jean Roncali<sup>\*,†</sup>

Groupe Systèmes Conjugués Linéaires, IMMO, UMR CNRS 6501, Université d'Angers, 2 Bd Lavoisier, 49045 Angers, France, Service Commun d'Analyses Spectroscopiques, 16 Bd Daviers, 49100 Angers, France, Groupe de Dynamique des Phases Condensées, UMR CNRS 5581, Université de Montpellier 2, 39095 Montpellier Cedex 5, France, and Departamento de Química Organica, ICMA, Universidad de Zaragoza, CSIC, E-50009 Zaragoza, Spain

pierre.frere@univ-angers.fr

Received March 11, 2003

Three series of thiophene-based  $\pi$ -conjugated oligomers built with different combinations of thiophene cycles and double bonds have been synthesized and characterized. The analysis of the chain length dependence of the electronic, electrochemical, and vibrational properties of the three series of oligomers has been carried out using cyclic voltammetry, UV-vis, IR, and Raman spectroscopies. These various investigations provide consistent results showing that incorporation of ethylenic linkages in an oligothiophene structure leads to a faster decrease of the HOMO-LUMO gap with chain extension due to the combined effects of enhanced planarity and lower overall aromatic character of the system. Although the incorporation of two consecutive double bonds in the system leads to a stabilization of the dicationic state, this structural modification does not produce the expected further decrease of the HOMO-LUMO gap at large chain extension. This phenomenon is discussed on the basis of an interplay between aromaticity and bond length alternation.

### Introduction

The unique electronic properties of linearly conjugated oligomers and polymers originate from a system of  $\pi$ -electrons extending over a large number of  $sp^2$  carbons. Full delocalization of  $\pi$ -electrons would result in carbon-carbon bonds of equal lengths, and chain extension should lead to the progressive closure of the HOMO-LUMO gap ( $\Delta E$ ). However, for these unidimensional systems, the electron-electron correlation combined with the electron-phonon coupling leads to an uneven distribution of  $\pi$ -electrons and hence to the development of alternate single and double bonds.<sup>1</sup> A major consequence of this process is that chain extension leads to the convergence of  $\Delta E$  toward a finite limit which directly depends on the specific chemical structure of the  $\pi$ -conjugated system.<sup>2</sup>

During the past decade, the chain-length dependence of many series of well-defined  $\pi$ -conjugated oligomers have been investigated in detail. Thus, extrapolation of

quantities such as absorption maximum or oxidation potential measured on oligomers of increasing chain length have been used to predict the ultimate properties of an ideal defect-free infinite polymer chain.<sup>3</sup> Examination of the data obtained for various series of (hetero)aromatic oligomers shows that both the convergence limit of  $\Delta E$  and the rate at which the system converges toward this limit depend on structural factors such as bond length alternation, planarity, and aromatic resonance energy of the (hetero)aromatic ring.<sup>2,3</sup>

In recent years, we have developed various series of extended oligothiophenevinylenes (nTVs).<sup>4</sup> Detailed analyses of the chain-length dependence of the electronic properties of these oligomers have shown that they present the smallest  $\Delta E$  value and longest convergence limit among all classes of known extended  $\pi$ -conjugated oligomers.<sup>4,5</sup> Indeed, the limitation of rotational disorder and the decrease of the overall aromaticity of the system associated with the thiophene/double bond alternation

\* To whom correspondence should be addressed. Fax: 33(0)2 41 73 54 05.

<sup>†</sup> Université d'Angers.

<sup>‡</sup> Service Commun d'Analyses Spectroscopiques.

<sup>§</sup> Université de Montpellier 2.

<sup>||</sup> Universidad de Zaragoza.

(1) Brédas, J. L.; Cornil, J.; Beljonne, D.; Dos Santos, D. A.; Shuai, Z. *Acc. Chem. Res.* **1999**, *32*, 267.

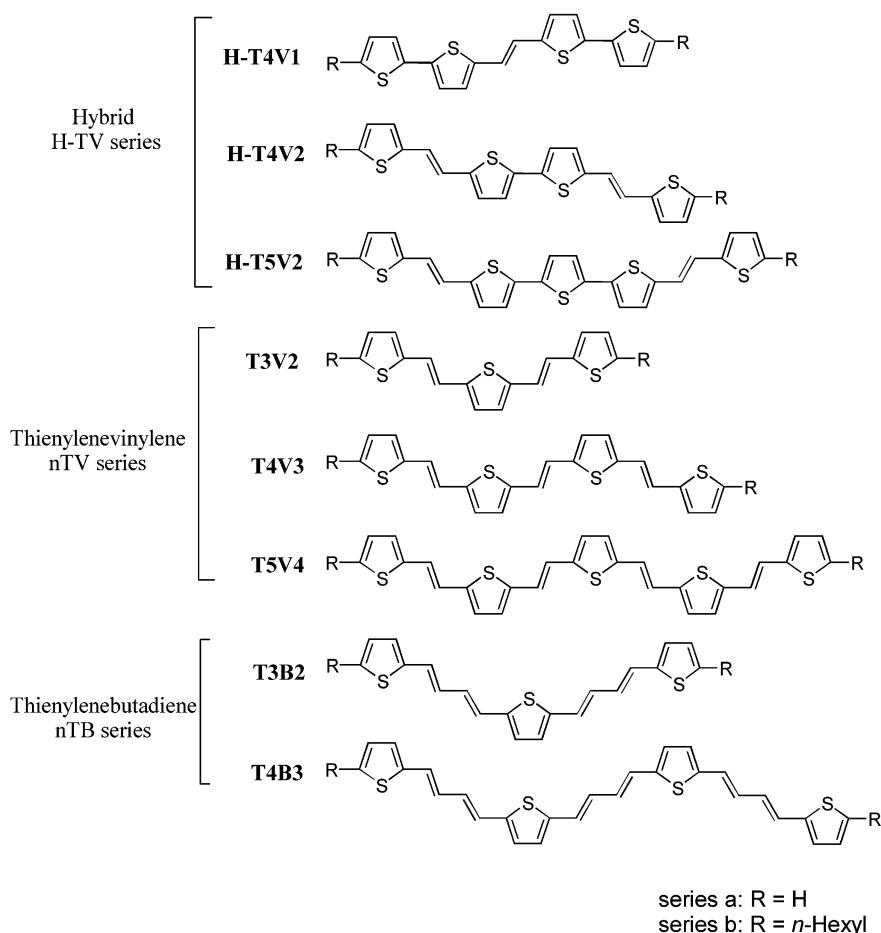
(2) Roncali, J. *Chem. Rev.* **1997**, *97*, 173.

(3) (a) *Electronic Materials: the Oligomer Approach*; Müllen, K., Wegner, G., Eds.; Wiley-VCH: Weinheim, 1997. (b) Martin, R. E.; Diederich, F. *Angew. Chem., Int. Ed.* **1999**, *38*, 1350. (c) Meier, H.; Stalmach, U.; Kolshorn, H. *Acta Polym.* **1997**, *48*, 379.

(4) (a) Elandaloussi, E. H.; Frère, P.; Richomme, P.; Orduna, J.; Garin, J.; Roncali, J. *J. Am. Chem. Soc.* **1997**, *119*, 10774. (b) Jestin, I.; Frère, P.; Blanchard, P.; Roncali, J. *Angew. Chem., Int. Ed.* **1998**, *37*, 942. (c) Jestin, I.; Frère, P.; Mercier, N.; Levillain, E.; Stievenard, D.; Roncali, J. *J. Am. Chem. Soc.* **1998**, *120*, 8150.

(5) Roncali, J. *Acc. Chem. Res.* **2000**, *33*, 147.

CHART 1



leads to a significant decrease of  $\Delta E$  compared to, e.g., oligothiophenes (nTs) containing the same number of  $sp^2$  carbons. On such a basis, it might be expected that insertion of additional double bonds between the thiophene rings could contribute to a further decrease of  $\Delta E$  at given chain lengths.

To investigate this question in more detail, three series of  $\pi$ -conjugated oligomers involving various combinations of thiophene rings and double bonds have been synthesized (Chart 1) and a comparative analysis of the chain length dependence of their electronic properties has been carried out using cyclic voltammetry, UV-vis, and vibrational spectroscopies.

## Results and Discussion

**Synthesis.** The synthesis of the various series of oligomers is depicted in Schemes 1–3. A McMurry reaction of aldehydes **2a** or **2b**, obtained by Vilsmeier formylation of bithiophenes **1a** or **1b**, gave compounds **H-T4V1** essentially as *E*-isomers. Recrystallization from EtOH/CHCl<sub>3</sub> gave pure *E*-isomer in 40% and 60% yield for **H-T4V1a** and **H-T4V1b**, respectively. Although the NMR spectra of hybrids **H-T4V1** do not allow to determine the configuration of the double bond, they suggest the presence of a pure isomer. Thus, the <sup>1</sup>H NMR spectra only show the expected singlet for ethylenic protons. On the other hand, the <sup>13</sup>C NMR spectrum of **H-T4V1b** only shows eight signals between 120 and 150

ppm corresponding to the  $sp^2$  carbons since, as demonstrated by HMQC experiments, the two carbons at the 3' and 4 positions of the thiophene rings are equivalent.

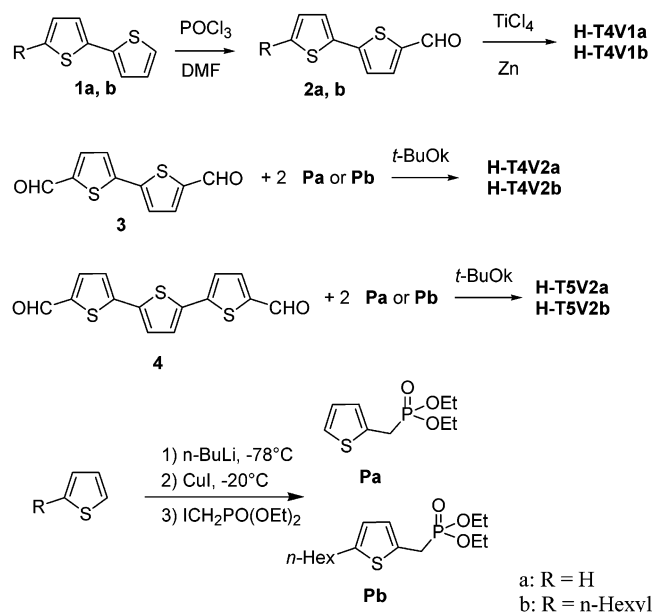
Compounds **H-T4V2** and **H-T5V2** were obtained by double Wittig–Horner olefination of diformyl bi- or terthiophene **3** and **4** with diethyl 2-thienylmethylphosphonate (**Pa**) or diethyl 2-(5-hexylthienyl)methylphosphonate (**Pb**) in the presence of *t*-BuOK at room temperature (Scheme 1). These phosphonates were obtained by a one-step reaction of diethyl iodomethylphosphonate on the corresponding 2-thienylcopper reagent.<sup>6</sup> In the <sup>1</sup>H NMR spectrum of **H-T4V2b** and **H-T5V2b** recorded in C<sub>6</sub>D<sub>6</sub>, the ethylenic protons appear as an AB doublet (<sup>3</sup>*J* = 15.7 Hz) pointing to the whole *trans* configuration of the molecules.

Unsubstituted nTVs **T3V2a**, **T4V3a**, and **T5V4a** were synthesized as already reported.<sup>7</sup> End-substituted **T3V2b**, **T4V3b**, and **T5V4b** have been obtained by 2-fold Wittig–Horner olefination of dialdehydes **5**, **6**, and **7** with phosphonate **Pb** (Scheme 2). Recrystallization from CHCl<sub>3</sub>–hexane gave pure *E*-isomers of **T3V2b**, **T4V3b**, and **T5V4b** in 70%, 60%, and 65% yield, respectively. The <sup>1</sup>H NMR spectrum of **T3V2b** and **T4V3b** shows the symmetrical ethylenic parts as AB systems with a  $\Delta\nu/J$  ratio of 3, leading to a *trans* coupling constant of the olefinic protons (<sup>3</sup>*J*) of 15.5 Hz. For **T5V4b**, the solvent

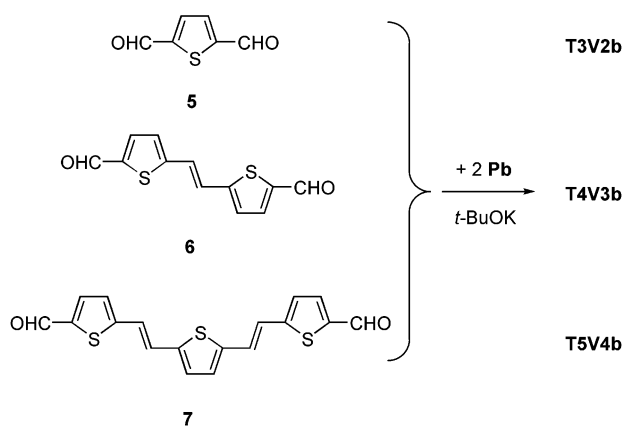
(6) Wang, C.; Dalton, L. R. *Tetrahedron Lett.* **2000**, *41*, 617.

(7) Nakayama, J.; Fujimori, T. *Heterocycles* **1991**, *32*, 991

## SCHEME 1



## SCHEME 2



shift effects observed in  $\text{C}_6\text{D}_6$  allows to distinguish ethylenic and aromatic protons. The ethylenic system connected to the terminal thiophenes appears as a AB doublet ( $\Delta\nu/J = 3$  and  $^3J = 15.4$  Hz), whereas the two magnetically equivalent central ethylenic linkages occur a sharp singlet corresponding to an  $\text{A}_2$  system.

Kossmehl and al. synthesized **T3B2a** by a Wittig reaction followed by isomerization with iodine to obtain the *all-trans* isomer.<sup>8</sup> To skip the isomerization step, we developed an alternative synthesis involving two successive Wittig–Horner olefinations. The first step involves the formation of the butadiene system by olefination of 2-thiophenecarbaldehyde **10** with phosphonate **Pc** bearing an ethylenic group (Scheme 3). Alcohol **9**, obtained by reduction of 2-thienylacrolein **8** with  $\text{NaBH}_4$ , was treated with  $\text{PBr}_3$  to yield the bromide derivative. Due to its high instability, this latter compound was immediately reacted with the anion diethyl phosphite to give phosphonate **Pc** in 65% yield for the two steps. Wittig–Horner olefination of 2-thienylacrolein with **Pc**, in the presence of *t*-BuOK, afforded **T2B1a** in 60%

yield. Vilsmeier formylation of **T2B1a** gave monoaldehyde **11** in 74% yield, while dialdehyde **12** was prepared in 56% yield by dilithiation followed by reaction with DMF. Wittig–Horner olefination of aldehyde **11** with **Pc** gave **T3B2a** in 74% yield.

Double olefination of dialdehyde **12** gave an unseparable mixture of **T3B2a** and **T4B3a**. In the presence of a strong base, dialdehyde **12** is quickly converted into monoaldehyde **11** by mono-decarbonylation. Then, a nucleophilic attack of the phosphonate anion on the mixture of **11** and **12** leads to **T3B2a** and **T4B3a**. Decarbonylation of a 2-thienylacrolein group by a strong base has already been observed by Cava et al. who concluded that this reaction was caused by the generation of an acylanion, followed by a loss of carbon monoxide.<sup>9</sup>

Because of the poor yield of diolefination with **Pc**, another route toward **T4B3a** and its soluble analogues **T3B2b** and **T4B3b** has been developed. This alternative approach involves first the formation of the acrolein system followed by olefination with phosphonates **Pa** or **Pb**. Thus, olefination of thienylacrolein with **Pa** afforded **T2B1a** in a better yield (85%) than the first route whereas two-fold olefination of 2,5-diacrolein-thiophene **13** with **Pb** gave **T3B2b** in 66% yield. Treatment of **T2B1a** with *n*-BuLi and 3-dimethylaminoacrolein gave bis-1,4-(2-thienylacrolein)butadiene **14** in 60% yield. Bis-olefination of **14** with **Pa** gave **T4B3a** while, **T4B3b** was obtained in 70% yield from **Pb**. Recrystallization from  $\text{CHCl}_3$  or  $\text{CHCl}_3$ –hexane, gave **T3B2a**, **T3B2b**, and **T4B3b** as pure *E*-isomers, but the poor solubility of **T4B3a** did not allow a correct purification.

The whole *trans* configuration of the various oligomers has been confirmed by 500 MHz  $^1\text{H}$  NMR. Although for the unsymmetrical monoaldehyde **11** the butadienic protons present easily identified AB or  $\text{AB}_2$  patterns, for compounds **12**, **14** and **T2B1a** an  $\text{AA}'\text{XX}'$  ( $J_{\text{XX}'} = 0$  Hz) pattern is observed in  $\text{C}_6\text{D}_6$  with  $\Delta\delta$  between the  $\text{AA}'$  and the  $\text{XX}'$  parts varying from 0.25 to 0.40 ppm. The coupling  $^3J_{\text{AX}} \approx 15.0$  Hz and  $^3J_{\text{AA}'} \approx 10.0$  Hz are characteristic of a *trans* configuration for each butadiene unit.

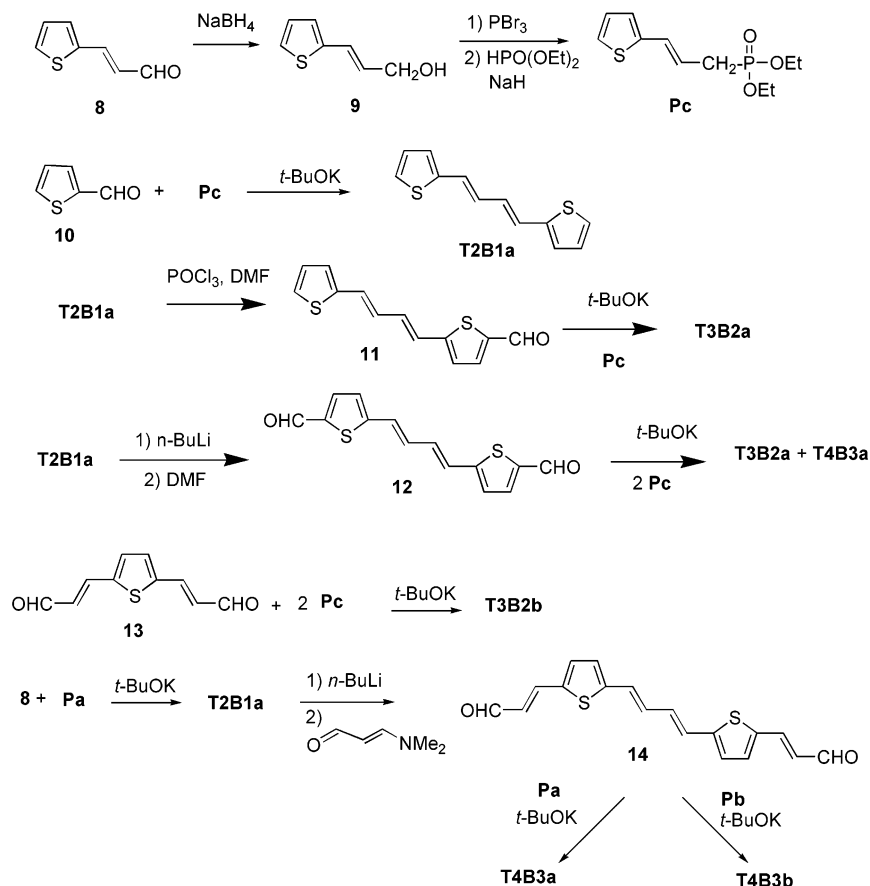
As shown in Figure 1 (top), the aromatic and ethylenic protons of **T3B2a** are easily identified on the spectrum recorded in  $\text{C}_6\text{D}_6$ . Protons of the butadiene system appear as three symmetrical multiplets centered at 6.65, 6.41, and 6.32 ppm, respectively, with a ratio of 2/1/1 in the integral sets. Even with the same apparent chemical shifts, protons H2 and H3 are magnetically inequivalent whereas the chemical shifts difference between H1 and H4 protons is only of 0.08 ppm. As these patterns are very similar to the  $\text{AA}'$  part of an  $\text{AA}'\text{XX}'$  system, the coupling constants given in Table 1 were evaluated with usual equations for a second order spectrum. The close agreement between the resulting theoretical spectrum (Figure 1, bottom) and the experimental spectrum strongly supports our interpretation.

For **T3B2b**, the overlap of the signals for H2 and H3 with those of the thiophenic protons does not allow an unequivocal assignment. However, owing to the similar resonance of H1 and H4 to those of **T3B2a**, the coupling

(8) Kossmehl, G.; Bohn, B.; Manecke, G. *Makromol. Chem.* **1976**, *177*, 1857.

(9) Mohanackrishnan, A. K.; Lakshmikantham, M. V.; McDougal, C.; Cava, M. P.; Baldwin, J. W.; Metzger, R. M. *J. Org. Chem.* **1998**, *63*, 3105.

SCHEME 3



constants were evaluated with the same method. The  $^3J_{\text{H1-H2}}$  and  $^3J_{\text{H3-H4}}$  thus obtained are close to 15.0 Hz which confirms the *all-trans* configuration of **T3B2a** and **T3B2b**. Finally, the configuration of **T4B3b** could not be directly deduced from its  $^1\text{H}$  NMR spectrum. However, only 14 resonances between 100 and 150 ppm appeared on its proton decoupled  $^{13}\text{C}$  NMR spectrum, as expected for a pure isomer.

Single crystals of **14** were obtained from slow evaporation of  $\text{CHCl}_3$  solution. The X-ray structure determination (Figure 2) clearly reveals the *all-trans* configuration of the butadiene spacer and of the acrolein system. To analyze the torsion and the bond length alternation of conjugated systems in the solid state, the X-ray data of **14**, **T2B1a**<sup>10</sup> (TB series), and **T3V2a**<sup>11</sup> (TV series) can be compared. In the TV series, the dithienylethylene molecule is nearly planar and the dihedral angle between the plane of the thiophene ring and that of the ethylene bonds is inferior to  $4^\circ$  in **T3V2a**. For **14**, the thiophene cycles present a twist angle of  $6^\circ$  with the fully planar butadiene unit and for **T2B1a** the angle reaches  $10^\circ$ . Bond length alternation calculated as the difference between the average length of single and double bonds for the 16 carbons of the conjugated systems is around 0.08 Å for both **T3V2a** and **14**.

**UV-vis Spectroscopy.** Figure 3 shows the electronic absorption spectra of the three series of end-substituted oligomers in  $\text{CH}_2\text{Cl}_2$ . The spectrum of **T4V1b** and **T4V2b** exhibits a discernible vibronic fine structure which vanishes for **T5V2b**. This effect suggests an increase of

the rotational disorder and hence a decrease of the rigidity of the  $\pi$ -conjugated with chain extension.

As already reported, the electronic absorption spectrum of nTVs exhibits a well resolved vibronic fine structure characteristic of planar rigid systems.<sup>4</sup> The constant energy spacing between the maximum of the lowest energy transition ( $\lambda_{0-0}$ ), main absorption band ( $\lambda_{\text{max}}$ ) and high energy band ( $1400\text{--}1500\text{ cm}^{-1}$ ) is consistent with a C=C stretching mode strongly coupled to the electronic structure.<sup>12</sup> The spectra of thienylenebutadiene (nTBs) are very similar to those of nTVs with however a slight enhancement of the resolution of the vibronic fine structure. Table 2 lists the main UV-vis data of the three series of oligomers. For each series, the +I inductive effect of the alkyl chains at the  $\alpha$ -position of the terminal thiophenes produces a small bathochromic shift of absorption bands. However, a closer examination shows that the magnitude of this electronic effect decreases with the lengthening of the  $\pi$ -conjugated system. This saturation effect already observed in highly extended nTVs end-substituted by dithiafulvenyl groups, has been attributed to the fact that as chain length increases,  $\Delta E$  becomes essentially determined by the topology of the  $\pi$ -conjugated system.<sup>13</sup> As expected, for each series, chain

(10) Buschmann, J. F.; Ruban, G. *Acta Crystallogr.* **1978**, *B34*, 1923

(11) Zobel, V. D.; Ruban, G. *Acta Crystallogr.* **1978**, *B34*, 1652.

(12) Rughooputh, S. D. D. V.; Hotta, S.; Heeger, A. J.; Wudl, F. *J. Polym. Sci.* **1987**, *25*, 1071.

(13) Jestin, I.; Frère, P.; Levillain, E.; Roncali, J. *Adv. Mater.* **1999**, *11*, 134.

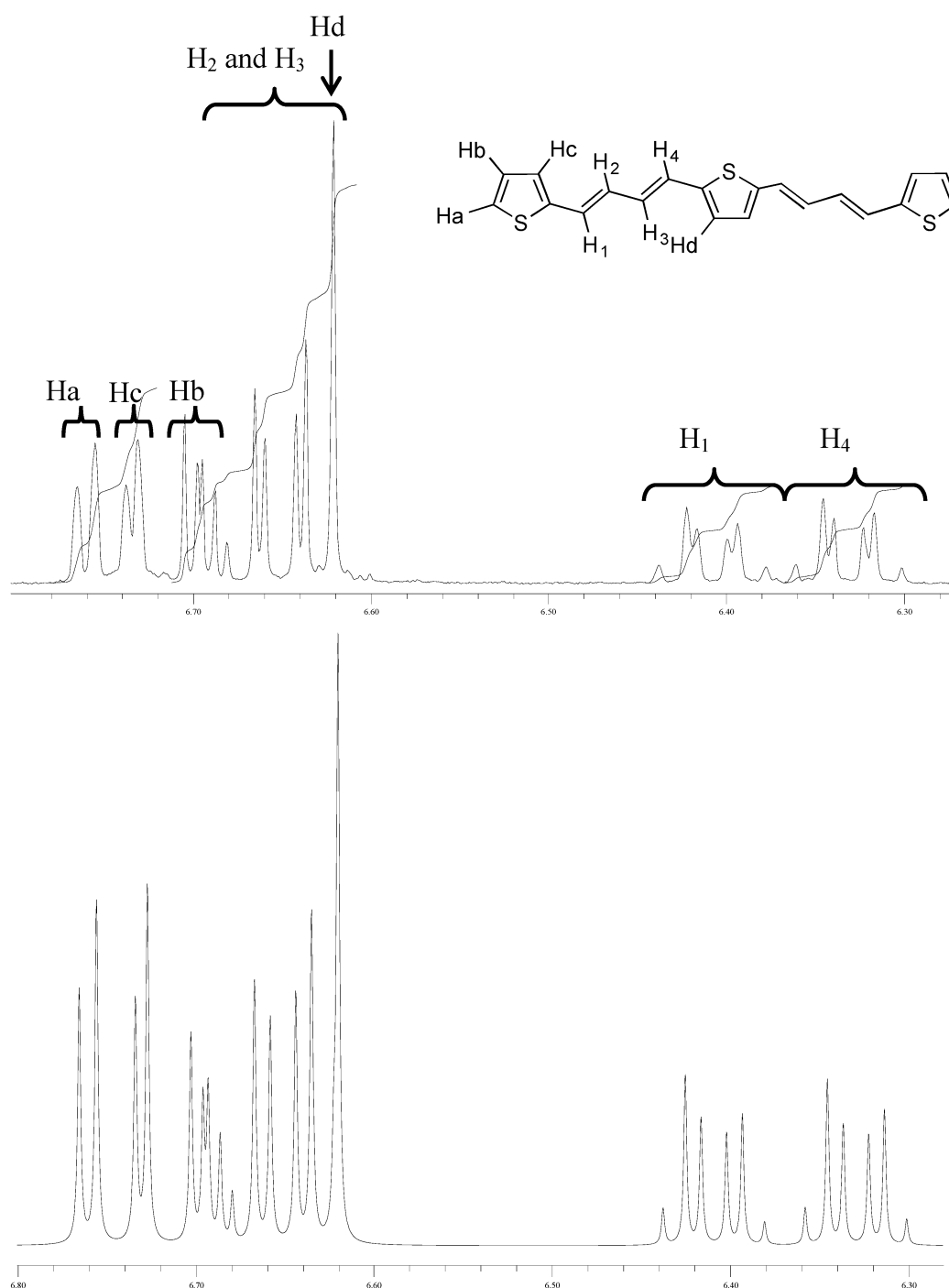


**FIGURE 1.** NMR spectra of **T3B2a**: (top) experimental spectrum in  $C_6D_6$ ; (bottom) theoretical spectrum.

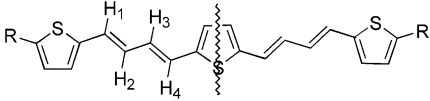
extension leads to a bathochromic shift of  $\lambda_{0-0}$  and hence to a decrease of  $\Delta E$ .

To compare the evolution of the absorption bands with the lengthening of the conjugated chain ( $Cn$ ), the plots of  $\lambda_{max}$  versus the reciprocal number of  $sp^2$  carbons has been reported in Figure 4 for each series and also for oligothiophene nTs.<sup>14</sup> Whereas  $\lambda_{max}$  scales linearly with  $1/Cn$  for nTVs and nTBs, a deviation from linearity is observed for nTs. The lowest slope is observed for nTs series and the highest for nTBs. However, at larger chain

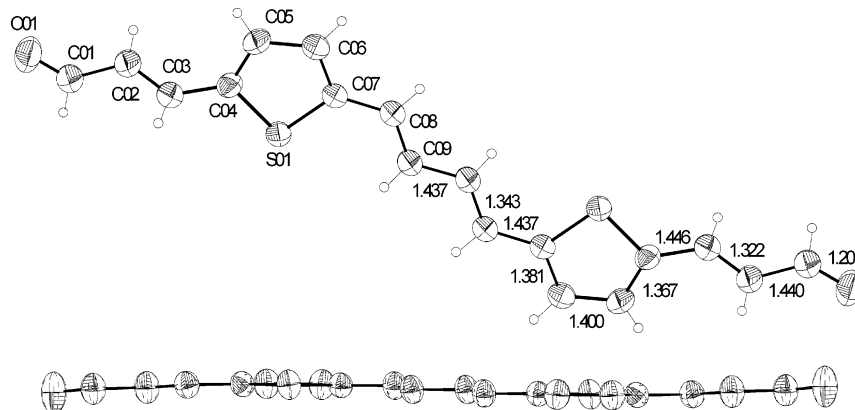
extension data for nTVs and nTBs are located on a common line and the two compounds corresponding to the longest chain length namely **T5V4b** and **T4B3b** ( $Cn = 28$   $sp^2$  carbons), show the same  $\lambda_{max}$  and  $\lambda_{0-0}$  of 493 and 527 nm respectively (Table 2).

The absolute value of  $\Delta E$  and the rate at which a  $\pi$ -conjugated system converges toward this limit depends on structural factors such as bond length alternation, planarity and aromaticity.<sup>2,3</sup> On this basis, the higher slopes obtained for nTVs and nTBs show that a given increment in chain length ( $Cn$ ) is more efficient to

(14) Bäuerle, P. In ref 3a, pp 105–197.

**TABLE 1.** Chemical Shifts and Coupling Constants for Protons of Butadiene Systems for **T3B2a** and **T3B2b**


compd	H1	H2	H3	H4
<b>T3B2a</b> (R = H)	$\delta = 6.41$ ppm $^3J_{H1-H2} = 15.1$ Hz $^4J_{H1-H3} = 0.9$ Hz	$\delta = 6.65$ ppm $^3J_{H2-H1} = 15.1$ Hz $^3J_{H2-H3} = 10.7$ Hz $^4J_{H2-H4} = 0.8$ Hz	$\delta = 6.65$ ppm $^3J_{H3-H4} = 15.2$ Hz $^3J_{H3-H2} = 10.7$ Hz $^4J_{H3-H1} = 0.9$ Hz	$\delta = 6.32$ ppm $^3J_{H4-H3} = 15.2$ Hz $^4J_{H4-H2} = 0.8$ Hz
<b>T3B2b</b> (R = Hex)	$\delta = 6.45$ ppm $^3J_{H1-H2} = 15.0$ Hz $^4J_{H1-H3} = 0.9$ Hz	multiplet between 6.62 and 6.74 ppm		$\delta = 6.35$ ppm $^3J_{H1-H2} = 15.0$ Hz $^4J_{H1-H3} = 0.9$ Hz

**FIGURE 2.** ORTEP view of (*E,E*)-1,4-bis[2-(3-oxo-2-propenyl)-5-thienyl]buta-1,3-diene **14** with bond lengths in Å.

reducing  $\Delta E$  than for the nTs series. This difference reflects the combined effects of enhanced planarity and lower overall aromaticity.

This major influence of ethylenic linkages is further confirmed by the location of the data for the hybrid compounds **H-T4V1**, **H-T4V2**, and **H-T5V2** between the plots corresponding to the nTs and nTVs/nTBs series. Conversely, the data for **H-T5V2** clearly show that despite the partial rigidification induced by the two ethylene linkages, the rotational disorder inherent to the central terthiophene core is prevalent, making this compound closer to the nTs series.

**Cyclic Voltammetry.** Table 3 lists the cyclic voltammetric (CV) data of the various oligomers. The CV of all compounds presents two reversible one-electron oxidation waves corresponding to the formation of the cation radical and dication at redox potential ( $E^0_1$ ) and ( $E^0_2$ ) except for **T3V2a** for which the second oxidation process is irreversible.

For each type of structure, introduction of hexyl chains at the  $\alpha$ -positions of the terminal thiophene rings produces a small negative shift of  $E^0_1$  and  $E^0_2$  and a decrease of the difference  $E^0_2 - E^0_1$  indicating that the +I inductive effect of the alkyl substituents raises the HOMO level and stabilizes the cationic state.

As expected, chain extension produces a shift of  $E^0_1$  toward negative potentials reflecting an increase of the HOMO level. Concurrently,  $E^0_2$  undergoes a negative shift of larger magnitude which results in a decrease of the difference  $E^0_2 - E^0_1$ . Thus, the CV of **T3B2b** presents two very close reversible oxidation peaks ( $\Delta E = 100$  mV) while for **T4B3b** the CV consists of a single broad redox system (Figure 5). Deconvolution reveals that this broad

oxidation wave involves in fact two very close one-electron oxidation steps. Comparison of the  $E^0_2 - E^0_1$  values for the three series of compounds shows that the decrease of the overall aromaticity of the system by replacing a thiophene cycle by one and then two double bonds leads to a dramatic decrease of  $E^0_2 - E^0_1$ . Conversely, the data for the hybrid compounds show that the presence of two or more adjacent thiophene rings produces the reverse effect with  $E^0_2 - E^0_1$  reaching values similar to those reported for nTs of comparable chain length.<sup>15</sup>

The magnitude of  $E^0_2 - E^0_1$  reflects the Coulombic repulsion between positive charges in the dicationic state. Since **T5V4** and **T4B3** have the same number of sp<sup>2</sup> carbons (28) the smaller  $E^0_2 - E^0_1$  value observed for **T4B3b** (40 mV vs 80 mV for **T5V4b**) shows that replacement of a thiophene ring by two ethylene linkages allows a better delocalization of the positive charges of the dication, thus leading to a weaker Coulombic repulsion. For short oligomers, the dication state is associated to a strong quinoid deformation with the structural changes located at the end of the molecule.<sup>16</sup> In this configuration, the decrease of the global aromatic character by the insertion of ethylenic bonds favors charge delocalization and the stabilization of the dication. The presence of the ethylenic bonds plays an important role on the energetic cost to produce the structural deformation of the conjugated chain between the two charges. Hence, direct two-electron transfer occurs for a chain length of 46 carbons

(15) Bäuerle, P. *Adv. Mater.* **1992**, *4*, 102.(16) Hapiot, P.; Kispert, L. D.; Konovalov, V. V.; Savéant, J.-M. *J. Am. Chem. Soc.* **2001**, *123*, 6669.

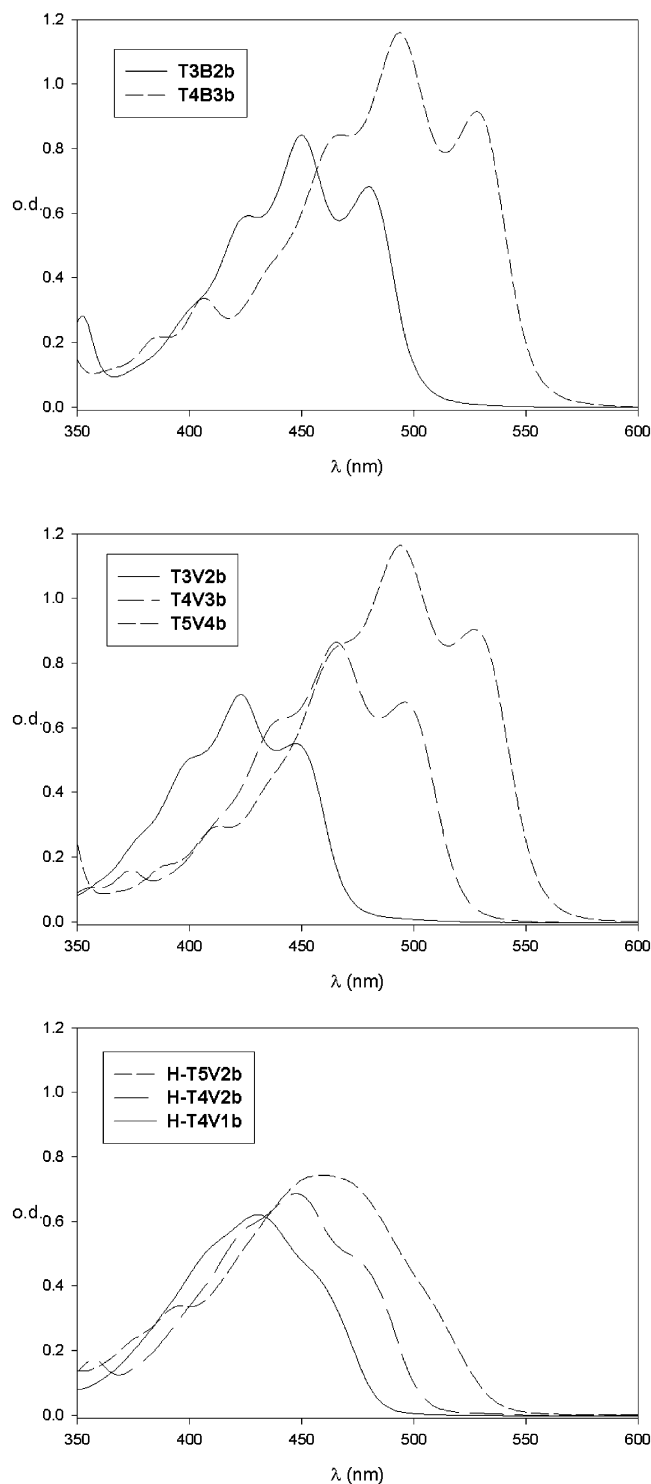


**FIGURE 3.** UV-vis spectra of the oligomers in  $\text{CH}_2\text{Cl}_2$ : (top) nTBb series; (middle) nTVb series; (bottom) H-TVb series.

in TVs<sup>4c</sup> and only for 20 carbons in oligoenes.<sup>16,17</sup> For **T4B2b**, the small value of  $\Delta E$  shows that the convergence of the two oxidation processes is close and should occur for a situation intermediate between nTVs and oligoenes.

**Vibrational Spectroscopy.** IR and Raman spectra of nTVs and nTBs have been recorded in the solid state.

(17) Heinze, J.; Tschuncky, P.; Smie, A. *J. Solid State Electrochem.* **1998**, *2*, 102.

**TABLE 2.** UV-vis Spectroscopic Data for the Various Oligomers in  $\text{CH}_2\text{Cl}_2$

compd	Cn	$\lambda_{\text{max}}$ , nm (eV)	$\lambda_{0-0}$ , nm (eV)
<b>H-T4V1a</b>	18	422 (2.94)	448 (2.77)
<b>H-T4V2a</b>	20	435 (2.85)	448 (2.77)
<b>H-T5V2a</b>	24	444 (2.79)	
<b>H-T4V1b</b>	18	431 (2.88)	456 (2.72)
<b>H-T4V2b</b>	20	449 (2.76)	477 (2.60)
<b>H-T5V2b</b>	24	458 (2.71)	
<b>T3V2a</b>	16	416 (2.98)	445 (2.79)
<b>T4V3a</b>	22	460 (2.70)	491 (2.53)
<b>T5V4a</b>	28	490 (2.53)	522 (2.38)
<b>T3V2b</b>	16	423 (2.93)	454 (2.73)
<b>T4V3b</b>	22	465 (2.67)	495 (2.51)
<b>T5V4b</b>	28	493 (2.52)	526 (2.36)
<b>T2B1a</b>	12	357 (3.47)	382 (3.25)
<b>T3B2a</b>	20	440 (2.82)	467 (2.66)
<b>T4B3a</b>	28	487 (2.55)	521 (2.38)
<b>T3B2b</b>	20	449 (2.76)	477 (2.60)
<b>T4B3b</b>	28	493 (2.52)	527 (2.35)

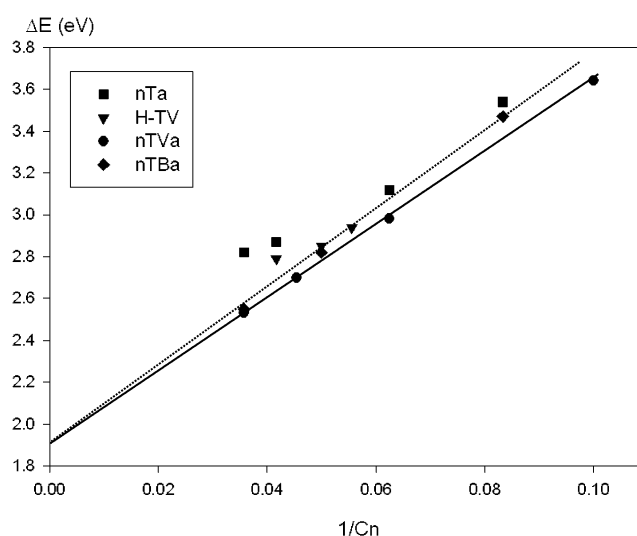


**FIGURE 4.** Plots of the absorption maximum versus the reciprocal number of  $\text{sp}^2$  carbons for the various series of conjugated oligomers (data for nTa series are taken from ref 14).

The analysis has been limited to the main characteristic bands which were compared to those of nTs and oligo-*p*-phenylenevinylene (nPVs) series. Table 4 lists the main IR frequencies and their assignment. The spectrum of nTVs presents strong bands around  $930\text{ cm}^{-1}$  involving a doublet for **T3V2b** and **T4V3b** and an intense broad band for **T5V4b**. By analogy with nPVs which present a strong absorption around  $970\text{ cm}^{-1}$ , these bands are assigned to the C-H out-of-plane wag of the trans vinylene.<sup>18</sup> For nPVs, the downshift of the frequency of the  $970\text{ cm}^{-1}$  band with chain extension has been attributed to a distortion of the conjugated chain.<sup>19</sup> In our case, the invariance of the frequency of the  $930\text{ cm}^{-1}$  band with chain extension suggests that the nTV chain is not subject to such a distortion.

The spectrum of **T5V4b** presents a broad band at  $797\text{ cm}^{-1}$  with a shoulder on the low-frequency side whereas

(18) (a) Tian, B.; Zerbi, G.; Müllen, K. *J. Chem. Phys.* **1991**, *95*, 3198.  
(b) Tian, B.; Zerbi, G.; Schenk, R.; Müllen, K. *J. Chem. Phys.* **1991**, *95*, 3191.

(19) Sakamoto, A.; Y. Furakawa, Y.; M. Tasumi, M. *J. Phys. Chem.* **1992**, *96*, 1490.

**TABLE 3.** Cyclic Voltammetric Data for Oligomers,  $10^{-4}$  M in 0.1 M  $\text{Bu}_4\text{NPF}_6/\text{CH}_2\text{Cl}_2$ , Scan Rate  $100 \text{ mV}\cdot\text{s}^{-1}$ , Reference  $\text{AgCl}/\text{Ag}$ 

compd	Cn	$E^0_1$ (V)	$E^0_2$ (V)	$E^0_2 - E^0_1$ (mV)
H-T4V1a	18	0.86	1.07 <sup>b</sup>	210
H-T4V2a	20	0.80	1.06	260
H-T5V2a <sup>a</sup>	24	0.73	0.97	240
H-T4V1b	18	0.74	0.92	180
H-T4V2b	20	0.71	0.90	190
H-T5V2b	24	0.68	0.87	170
T3V2a	16	0.87	1.13 <sup>b</sup>	260
T4V3a	22	0.74	0.92	180
T3V2b	16	0.76	0.97	220
T4V3b	22	0.67	0.80	130
T5V4b	28	0.62	0.70	80
T3B2a	20	0.76	0.92	160
T4B3a <sup>a</sup>	28	0.62	0.70	70
T3B2b	20	0.67	0.77	100
T4B3b	28	0.60	0.64	40

<sup>a</sup> Saturated solution. <sup>b</sup> Irreversible peak.

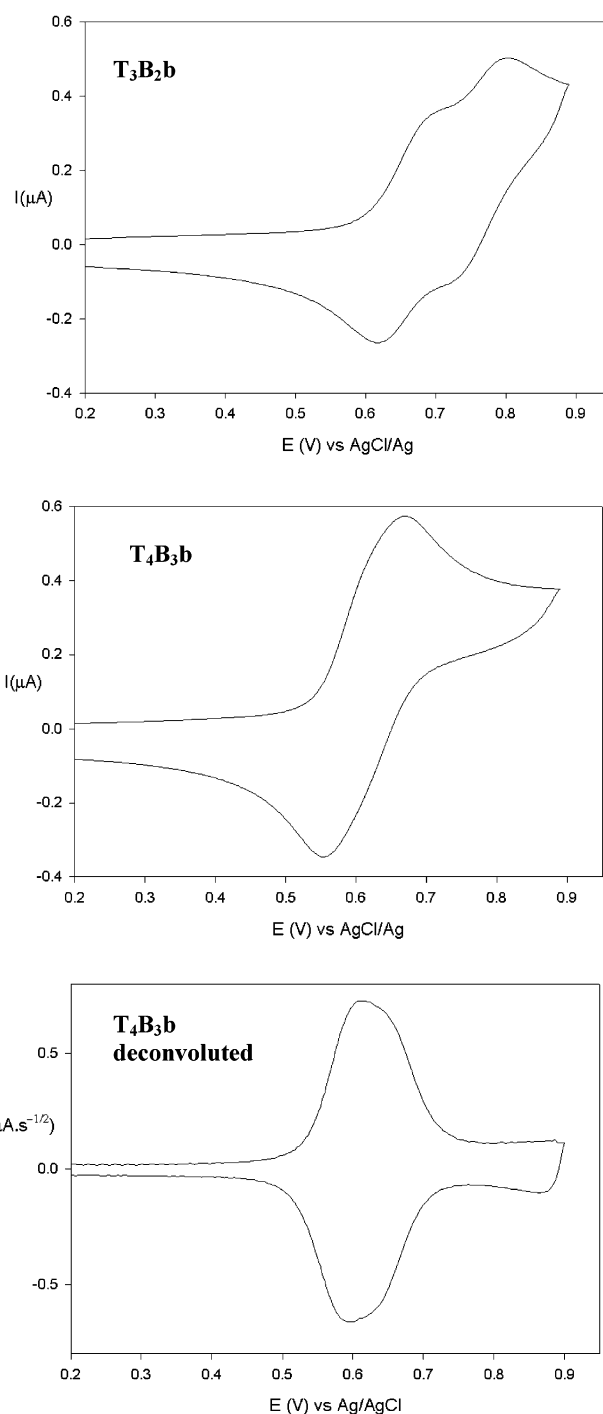
that of **T4V3b** and **T3V2b** shows an intense narrow band at  $800 \text{ cm}^{-1}$  and two well-defined weak peaks at  $780$  and  $770 \text{ cm}^{-1}$ . These bands can be assigned to the C–S vibrations and C–H out-of-plane mode of the  $\beta$ -carbon of the thiophene cycles.<sup>20</sup> As shown in Scheme 4, three different conformers corresponding to anti and syn conformations are possible for **T3V2** while the number goes up to 10 for **T5V4**. Indeed, a syn–anti form of **T3V2a** has been observed in the crystallographic structure<sup>11</sup> and it is likely that for longer nTVs, a mixture of the different conformers exists in the solid state which could account for the observed broadening of the IR bands. The effects of this conformational variability on the vibrational spectrum have been analyzed in the case of nTs.<sup>21</sup>

The IR spectrum of nTBbs presents a strong band around  $970 \text{ cm}^{-1}$  corresponding to the C–H out-of-plane wag of the *trans*-vinylene linkage. The frequency increases from  $970 \text{ cm}^{-1}$  for **T3B2b** to  $976 \text{ cm}^{-1}$  for **T4B3b** indicating that chain extension does not induce a severe torsion of the  $\pi$ -conjugated system. As noted by Kossmehl, the presence of a cis double bond in the structure of **T2B1a**, results in an intense band about  $930 \text{ cm}^{-1}$ .<sup>8</sup> The absence of such a band in the spectrum of nTBs confirms, in agreement with NMR data, the all-*trans* configuration of the molecules. The C–S vibrations and the C–H out-of-plane mode occur as two bands at  $823$  and  $800 \text{ cm}^{-1}$ . A strong and broad band is observed at  $800 \text{ cm}^{-1}$  in **T4B3b**, in contrast with **T3B2b** which displays three resolved weak bands centered around  $787 \text{ cm}^{-1}$ . Again, the increase of the number of possible conformers when going from **T3B2** to **T4B3** can explain the broadening of this band.

Raman spectroscopy has been widely used to analyze the chain length dependence of the effective conjugation length in linear  $\pi$ -conjugated systems. Previous work on oligomeric conjugated systems of homogeneous structure such as oligoenes have established a linear dependence

(20) (a) Hernandez, V.; Casado, J.; Ramirez, F. J.; Zotti, G.; Hotta, S.; Lopez Navarrete, J. T. *J. Chem. Phys.* **1996**, *104*, 9271. (b) Hernandez, V.; Kanamitsu, Y.; Lopez Navarrete, J. T. *J. Raman Spectrosc.* **1998**, *29*, 617.

(21) Millefiori, S.; Alparone, A.; Millefiori, A. *J. Heterocycl. Chem.* **2000**, *37*, 847.

**FIGURE 5.** Cyclic voltammograms of nTBb oligomers  $10^{-4}$  mol  $\text{L}^{-1}$  in 0.1 m  $\text{Bu}_4\text{NPF}_6/\text{CH}_2\text{Cl}_2$ , scan rate  $100 \text{ mV s}^{-1}$ ; (top) **T3B2b**; (middle) **T4B3b**; (bottom) **T4B3b** deconvoluted.

of the Raman shifts of resonantly coupled mode with the inverse conjugation length. For oligoenes involving 6 to 24  $\text{sp}^2$  carbons, the C=C stretching mode was found to shift by  $130 \text{ cm}^{-1}$ .<sup>22</sup> A more recent work on oligopyrroles has shown that the so-called  $\mathcal{A}$  mode near  $1500 \text{ cm}^{-1}$  shifts by  $45 \text{ cm}^{-1}$  when increasing chain length from 3 to 7 pyrrole rings<sup>23</sup> while for nTs oligomers practically no dispersion is observed with increasing the chain length.<sup>24</sup>

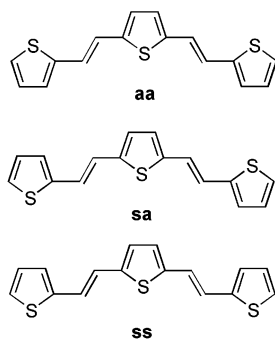
(22) Schaffer, H. E.; Chance, R. R.; Silbey, R. J.; Knoll, K.; Schrock, R. R. *J. Chem. Phys.* **1991**, *94*, 4161.



TABLE 4. IR Frequencies

compd	C–H out of plane wag for the vinylene units (cm <sup>-1</sup> )	C–S and C–H out of plane for the thiophene cycle (cm <sup>-1</sup> )
<b>T3V2b</b>	933 (st)	800 (st)
	930 (st)	780 (m)
		770 (m)
<b>T4V3b</b>	935 (st)	800 (st)
	930 (st)	780 (m)
		770 (m)
<b>T5V4b</b>	930 (st)	797 (st)
<b>T3B2b</b>	broad signal	broad signal
	970 (st)	827 (m)
		787 (m)
<b>T4B3b</b>		broad signal
	975 (st)	795 (m)
		821 (m)
		broad signal

SCHEME 4



The Raman spectra of nTVs and nTBs have been recorded using 514.5 or 647.1 nm excitation line. As for others  $\pi$ -conjugated oligomers, the Raman spectra are rather simple despite the complex chemical structure. In each oligomer a strong band assigned to the C–H cycle bending in plane vibration, appears at 1044 cm<sup>-1</sup>.

The C=C stretching region between 1200 and 1650 cm<sup>-1</sup> of the Raman spectrum of nTVs and nTBs exhibits two main bands around 1400 and 1600 cm<sup>-1</sup> corresponding to C=C stretching in thiophene ring deformation and C=C stretching in ethylene linkage, respectively (Table 5). The thiophene C=C stretching frequency moves downshifts by 16 cm<sup>-1</sup> between **T3V2b** and **T5V4b** while the vinylic (C=C) stretching downshifts by 10 cm<sup>-1</sup>. The correlated shifts of these two C=C modes with chain extension confirms that both “aromatic” and ethylenic double bonds contribute to  $\pi$ -electron delocalization.

The Raman spectra of the nTBs are more complex and show, in addition to the main bands observed in the TVs spectra, intense bands around 1130 cm<sup>-1</sup> assigned to the C–C stretching of the butadiene units (short polyene chain) (Table 5). Chain extension results in a downshift of the main bands corresponding to the  $\nu$ (C=C) modes of both the thiophene cycle (from 1437 to 1417 cm<sup>-1</sup> for **T3B2b** and **T4B3b** respectively) and of the vinylene linkages (from 1591 to 1587 cm<sup>-1</sup>). Again, these concomitant shifts reflect the coupling of the two types of double bonds of the  $\pi$ -conjugated system.

Figure 6 shows plots of the two types of C=C stretching frequency versus 1/C<sub>n</sub> for nTVs and nTBs. Although data

for nTBs are limited to a couple of points, comparison of the chain length dependence of the two types of C=C stretching frequencies reveals two different behaviors. For both nTVs and nTBs thiophenic C=C stretching data are located on the same straight line and scale linearly with 1/C<sub>n</sub>. Conversely, data corresponding to the vinylic C=C stretching frequencies for nTVs and nTBs follow two parallel lines, for a given C<sub>n</sub> value, the nTBs peaks are observed at lower wavenumbers. These contrasting behaviors suggest that the increase of the number of double bonds between the thiophene rings results in the creation of a short polyenic segment in which the behavior typical to polyenes, namely the dimerization becomes possible.

## Conclusion

Three series of extended  $\pi$ -conjugated systems of well-defined structure and geometry built up on various combinations of thiophene rings and double bonds have been synthesized and characterized. A comparative analysis of the chain-length dependence of the optical, and electrochemical properties of these various systems has shown that, as expected, chain extension results in a decrease of the HOMO–LUMO gap and in an increase of the HOMO level. The results obtained with the various series of oligomers provide a coherent picture showing that the incorporation of double bonds in an oligothiophene structure leads to faster decrease of the HOMO–LUMO gap with chain extension due to the synergistic effects of enhanced planarity and lower overall aromatic character. However, a further addition of ethylenic bonds by insertion of butadiene units between the thiophene rings does not produce the expected further narrowing of the gap. These results lead to the conclusion that the major effect of the ethylenic linkage concerns the planarization of the  $\pi$ -conjugated system by suppression of the rotational disorder inherent to oligothiophenes. Consequently, while contributing to decrease the overall aromatic character of the system, the incorporation of second double bond brings some freedom to the system which begins to behave as a “short polyene” in which small changes in bond length alternation become possible. In other words, the small decrease of the overall aromaticity associated with the insertion of an additional double bond is counter-balanced by an increase of the vibrational freedom.

These various sets of results thus definitively confirm that nTVs exhibit the smallest HOMO–LUMO gap among extended  $\pi$ -conjugated oligomers.

## Experimental Section

<sup>1</sup>H and <sup>13</sup>C spectra were recorded on a spectrometer operating at 500 MHz and 125.7 MHz respectively.  $\delta$  are given in ppm (relative to TMS) and *J* values in Hz. Cyclic voltammetry experiments were performed under dry nitrogen atmosphere. Working electrode (Pd disk) and counter electrode (Pt wire) were used, all potentials refer to AgCl/Ag as reference electrode. EI mass spectra were obtained at 70 eV and accurate mass measurements were performed at 10000 resolution (peak width at 5% height) using PFK as internal reference. Room-temperature micro-Raman experiments (x50 objective) were measured using Ar<sup>+</sup>–Kr<sup>+</sup> ion laser lines (514.5 and 647.1 nm) in the backscattering geometry on a spectrometer equipped with a liquid nitrogen cooled CCD detector. In all these

(23) Zerbi, G.; Veronelli, M.; Martina, S.; Schlütter, A.-D.; Wegner, G. *Adv. Mater.* **1995**, *5*, 385.

(24) Hernandez, V.; Castiglioni, C.; Del Zoppo, M.; Zerbi, G. *Phys. Rev. B*, **1994**, *50*, 9815.

TABLE 5. Raman Frequencies

compd	C–H bending (in plane) (cm <sup>-1</sup> )	C=C stretching (thiophene) (cm <sup>-1</sup> )	C=C stretching (vinylene) (cm <sup>-1</sup> )	C–C stretching (butadiene) (cm <sup>-1</sup> )
<b>T3V2b</b>	1044 (st)	1434 (st)	1603 (st)	
<b>T4V3b</b>	1044 (st)	1424 (st)	1596 (st)	
<b>T5V4b</b>	1045 (w)	1418 (st)	1593 (w)	
<b>T3B2b</b>	1044 (st)	1427 (sh)	1591 (st)	1139 (st)
		1437 (st)	1600 (w)	
		1468 (m)		
<b>T4B3b</b>	1045 (w)	1418 (st)	1587 (st)	1135 (m)
		1437 (m)	broad signal	1162 (m)
		1470 (m)		1189 (m)

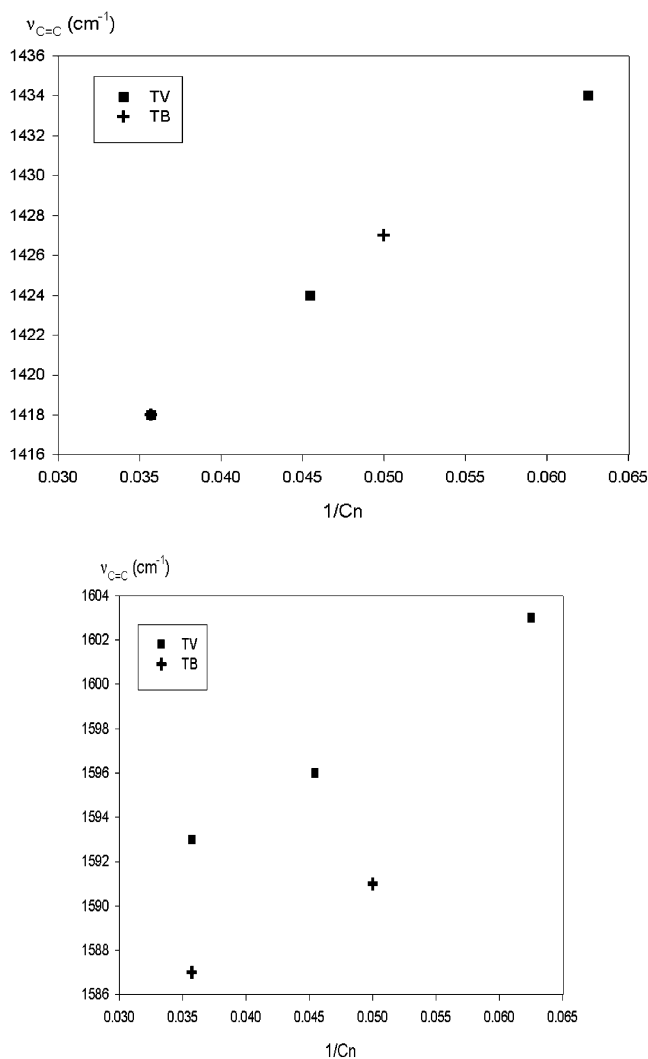


**FIGURE 6.** Shift of the C=C stretching mode vs reciprocal chain length for nTVbs and nTBbs: (top) thiophene C=C stretching; (bottom) vinylic C=C stretching.

experiments, the average laser power density was kept below 50 mW/mm<sup>2</sup> in order to minimize the local heating and to avoid sample degradation. Room-temperature IR transmission was carried out on samples pelletized with KBr using a fast-scan Fourier transform spectrometer. The investigated frequency range was 450–4000 cm<sup>-1</sup>. The resolution was fixed at 2 cm<sup>-1</sup>.

2-Thiophenecarbaldehyde and 2-hexylthiophene were purchased and used as received. Dialdehyde derivatives with thiophene (5), bithiophene (3), terthiophene (4), and thienylenevinylene (6 and 7) units as spacer were synthesized by a *n*-BuLi–DMF sequence.<sup>25</sup> Bithiophene **1a** and **1b** were obtained from Kumada or Stille coupling. 2-(3-Oxo-1-propenyl)-

thiophene **8** and 2,5-bis(3-oxo-1-propenyl)thiophene **13** were synthesized by Wittig oxopropenylation with 1,3-dioxan-2-ylmethyltributylphosphorane on the corresponding mono- or dialdehyde.<sup>25</sup>

**3-(2-Thienyl)-2-propenol (9).** To a solution of 2-(3-oxo-1-propenyl)thiophene **8** (3.3 g) in 40 mL of CH<sub>2</sub>Cl<sub>2</sub>/MeOH (1/1) at 0 °C was added portionwise NaBH<sub>4</sub> (0.9 g), and the mixture was allowed to warm at room temperature and stirred for 30 mn. After addition of water (30 mL), the mixture was extracted with twice 20 mL of dichloromethane. The organic phases were dried over MgSO<sub>4</sub> and evaporated in vacuo. The resulting oil was distilled under reduced pressure (0.2 mbar, 101–102 °C) to give a clear yellow oil (3.0 g, 88% yield): <sup>1</sup>H NMR (CDCl<sub>3</sub>) δ 7.15 (dd, 1H, <sup>3</sup>J = 3.5 Hz, <sup>3</sup>J = 2.3 Hz); 6.95 (m, 2H), 6.75 (dd, 1H, <sup>3</sup>J = 15.5 Hz, <sup>4</sup>J = 1.4 Hz); 6.18 (td, 1H, <sup>3</sup>J = 5.6 Hz, <sup>3</sup>J = 15.5 Hz); 4.26 (dd, 2H, <sup>3</sup>J = 5.6 Hz, <sup>4</sup>J = 1.4 Hz); 2.01 (s, 1H).

**Diethyl [3-(2-Thienyl)-2-propenyl]phosphonate (Pc). Preparation of the Solution of Anion of Diethyl Phosphite.** Under N<sub>2</sub> atmosphere, a suspension of 2.8 g of NaH (60% in oil, washed with twice 10 mL of dry THF) in 10 mL of THF was cooled at –15 °C. A solution of 8 mL of diethyl phosphite in 40 mL of dry THF was added dropwise over a period of 1 h. After 1 h of stirring, the mixture was allowed to stand at –5 °C.

**Preparation of Phosphonate.** To a solution of 2.95 g of alcohol **9** in benzene (20 mL)–toluene (10 mL) cooled at –20 °C was added 3.5 mL of PBr<sub>3</sub>, and the mixture was allowed to warm at –10 °C. The solution of bromide derivative was rapidly transferred in a dropping funnel and was added to the solution of anion of diethyl phosphite at –10 °C. The mixture was allowed to warm at room temperature and stirred for 2 h. After addition of water (100 mL), the mixture was extracted with twice 50 mL of Et<sub>2</sub>O. The organic phase was separated, and the aqueous phase was extracted with Et<sub>2</sub>O. The organic phases were dried over MgSO<sub>4</sub> and evaporated in vacuo. Flash chromatography on silica gel (AcOEt/CH<sub>2</sub>Cl<sub>2</sub> 2/1) afforded oil which was distilled with a Kugelrohr apparatus (0.2 mbar, 173 °C) to give a clear yellow oil (3.7 g, 74% yield): MS (EI) *m/z* = 260 [M<sup>+</sup>]; <sup>1</sup>H NMR (CDCl<sub>3</sub>) δ 7.10 (d, <sup>3</sup>J = 4.7 Hz, 1H), 6.9 (m, 2H), 6.65 (dd, <sup>3</sup>J = 15.5 Hz, <sup>4</sup>J<sub>H-P</sub> = 5.1 Hz, 1H), 5.9 (td, <sup>3</sup>J = 15.5 Hz, <sup>3</sup>J<sub>H-P</sub> = 7.7 Hz, 1H), 4.10 (m, 4H), 2.70 (dd, <sup>3</sup>J = 7.7 Hz, <sup>2</sup>J<sub>H-P</sub> = 22.3 Hz, 2H), 1.30 (m, 6H).

**General Procedure for the Vilsmeier Reaction.** To a solution of 2.3 mmol of bithiophene derivatives **1a,b** or **T2B1a** and 0.25 mL of DMF in 25 mL of dry dichloroethane, in a round-bottomed flask kept under a nitrogen atmosphere, was added 0.26 mL of POCl<sub>3</sub>, and then the mixture was refluxed for 8 h. After cooling to room temperature, 1 M sodium acetate was added to neutrality and the mixture was stirred vigorously for 1 h. The solution was extracted with dichloromethane, and the organic phase was dried over Na<sub>2</sub>SO<sub>4</sub>. After evaporation of the solvent, the crude product was purified by chromatography on silica gel (eluent, CH<sub>2</sub>Cl<sub>2</sub>).

(25) (a) Feringa, B. L.; Hulst, R.; Rikers, R.; Brandsma, L. *Synthesis* **1998**, 316. (b) Nakayama, J.; Fujimori, T.; *Sulfur Lett.* **1990**, 11, 29. (c) Elandaloussi, E. H.; Frère, P.; Roncali, J.; Richomme, P.; Jubault, M.; Gorgues, A. *Adv. Mater.* **1995**, 7, 390.

**(E,E)-1-(2-Thienyl)-4-(5-formyl-2-thienyl)buta-1,3-diene (11):** orange powder (74% yield); mp 116 °C; <sup>1</sup>H NMR (CDCl<sub>3</sub>) δ 9.83 (s, 1H), 7.63 (d, 1H, <sup>3</sup>J = 3.8 Hz), 7.24 (d, 1H, <sup>3</sup>J = 5.0 Hz), 7.06 (d, 2H, <sup>3</sup>J = 3.8 Hz), 7.00 (dd, 1H, <sup>3</sup>J = 5.0 Hz, <sup>3</sup>J = 3.8 Hz), 6.91 (dd, 1H, <sup>3</sup>J = 15.1 Hz, <sup>3</sup>J = 10.5 Hz), 6.89 (d, 1H, <sup>3</sup>J = 15.3 Hz), 6.74 (d, 1H, <sup>3</sup>J = 15.1 Hz), 6.70 (dd, 1H, <sup>3</sup>J = 15.3 Hz, <sup>3</sup>J = 10.5 Hz); C<sub>13</sub>H<sub>10</sub>OS<sub>2</sub>, MS (EI) *m/z* = 246 [M<sup>+</sup>].

**5-Formyl-2,2'-bithiophene (2a):** yellow powder (80% yield); mp 58–59 °C (lit.<sup>27</sup> mp 57–59 °C); <sup>1</sup>H NMR (CDCl<sub>3</sub>) δ 9.86 (s, 1H), 7.67 (d, 1H, <sup>3</sup>J = 3.9 Hz), 7.35 (d, 2H, <sup>3</sup>J = 4.4 Hz), 7.25 (d, 1H, <sup>3</sup>J = 3.9 Hz), 7.10 (t, 1H, <sup>3</sup>J = 4.4 Hz); C<sub>9</sub>H<sub>6</sub>OS<sub>2</sub>, MS (EI) *m/z* = 194 [M<sup>+</sup>].

**5-Formyl-5'-*n*-hexyl-2,2'-bithiophene (2b):** yellow oil (85% yield); <sup>1</sup>H NMR (CDCl<sub>3</sub>) δ 9.85 (s, 1H), 7.65 (d, 1H, <sup>3</sup>J = 4.0 Hz), 7.18 (d, 1H, <sup>3</sup>J = 3.8 Hz), 7.16 (d, 1H, <sup>3</sup>J = 3.9 Hz), 6.78 (d, 1H, <sup>3</sup>J = 3.8 Hz); C<sub>15</sub>H<sub>18</sub>OS<sub>2</sub>, MS (EI) *m/z* = 278 [M<sup>+</sup>].

**(E,E)-1,4-Bis(5-formyl-2-thienyl)buta-1,3-diene (12):** To a solution of **T2B1a** (0.634 g, 2.9 mmol) in 100 mL of Et<sub>2</sub>O + 50 mL of THF, cooled at 0 °C under nitrogen, was added dropwise a solution of *n*-BuLi 1.6 M in hexane (5.5 mL, 3 equiv). The mixture was stirred at 0 °C for 2 h, and 7 mL (90 mmol) of DMF was added. After 2 h of stirring at ambient temperature and hydrolysis with 3 N aqueous NH<sub>4</sub>Cl, the mixture was extracted with CH<sub>2</sub>Cl<sub>2</sub>, and the organic phases were washed with water, dried over MgSO<sub>4</sub>, and evaporated. Column chromatography of the residue (silica gel, CH<sub>2</sub>Cl<sub>2</sub>/ethyl acetate 10:1) gave a red solid (0.424 g, 56% yield): mp 200 °C (lit.<sup>28</sup> mp 200 °C); <sup>1</sup>H NMR (C<sub>6</sub>D<sub>6</sub>) δ 9.47 (s, 2H), 6.82 (d, 2H, <sup>3</sup>J = 3.9 Hz), 6.45 (d, 2H, <sup>3</sup>J = 3.9 Hz), 6.40 (2H, AA', <sup>3</sup>J<sub>AX</sub> = 15.3 Hz, <sup>3</sup>J<sub>AA'</sub> = 10.5 Hz, <sup>3</sup>J<sub>AX}</sub> = 0.9 Hz, <sup>3</sup>J<sub>XX'} = 0 Hz), 6.01 (2H, AA', <sup>3</sup>J<sub>AX} = 15.3 Hz, <sup>3</sup>J<sub>AA'</sub> = 10.5 Hz, <sup>3</sup>J<sub>AX}</sub> = 0.9 Hz, <sup>3</sup>J<sub>XX'} = 0 Hz); C<sub>14</sub>H<sub>10</sub>O<sub>2</sub>S<sub>2</sub>, MS (EI) *m/z* = 274 [M<sup>+</sup>].</sub></sub></sub>

**(E,E)-1,4-Bis(5-acrolein-2-thienyl)buta-1,3-diene (14):** To the solution of 2 mmol of dilithiated derivative of compound **T2B1a** was added 0.7 mL (7 mmol) of 3-dimethylaminoacrolein dropwise at 0 °C under nitrogen. After 4 h of stirring at ambient temperature and hydrolysis with 3 N aqueous NH<sub>4</sub>-Cl, the usual workup and column chromatography (silica gel, CH<sub>2</sub>Cl<sub>2</sub>/ethyl acetate 10:1) gave a red solid (220 mg, 33% yield): mp 191 °C; <sup>1</sup>H NMR (C<sub>6</sub>D<sub>6</sub>) δ 9.35 (d, 2H, <sup>3</sup>J = 7.4 Hz), 6.67 (d, 2H, <sup>3</sup>J = 15.6 Hz), 6.56 (d, 2H, <sup>3</sup>J = 3.8 Hz), 6.49 (2H, AA', <sup>3</sup>J<sub>AX} = 15.1 Hz, <sup>3</sup>J<sub>AA'</sub> = 10.3 Hz, <sup>3</sup>J<sub>AX}</sub> = 0.7 Hz, <sup>3</sup>J<sub>XX'} = 0 Hz), 6.47 (d, 2H, <sup>3</sup>J = 3.8 Hz), 6.40 (dd, 2H, <sup>3</sup>J = 15.6 Hz, <sup>3</sup>J = 7.4 Hz), 6.22 (2H, AA', <sup>3</sup>J<sub>AX} = 15.1 Hz, <sup>3</sup>J<sub>AA'</sub> = 10.3 Hz, <sup>3</sup>J<sub>AX}</sub> = 0.7 Hz, <sup>3</sup>J<sub>XX'} = 0 Hz); <sup>13</sup>C NMR (CDCl<sub>3</sub>) δ 192.6, 147.4, 143.9, 138.5, 133.5, 130.7, 128.0, 127.1, 126.5; C<sub>18</sub>H<sub>14</sub>O<sub>2</sub>S<sub>2</sub>, MS (EI) *m/z* = 326 [M<sup>+</sup>].</sub></sub></sub></sub>

**General Procedure for the Mc Murry Reaction.** To a suspension of low valent Ti prepared from TiCl<sub>4</sub> (0.66 mL, 6 mmol) and Zn (0.78 g, 12 mmol) in 30 mL of dry THF under N<sub>2</sub> at 0 °C was added a dry solution of aldehyde **1a** or **1b** (5 mmol) in 10 mL of THF. After 2 h of refluxing, the mixture was cooled to room temperature, poured into water, and then extracted with CH<sub>2</sub>Cl<sub>2</sub>. The organic phase was washed with water and dried over MgSO<sub>4</sub>. After solvent removal, the crude solid was recrystallized.

**1,2-Bis[2-(2-thienyl)-5-thienyl]ethene (H-T4V1a):** orange powder recrystallized from ethanol; yield 40%; mp 190 °C dec; <sup>1</sup>H NMR (CDCl<sub>3</sub>) δ 7.22 (d, 2H, <sup>3</sup>J = 5.0 Hz), 7.18 (d, 2H, <sup>3</sup>J = 3.5 Hz), 7.07 (d, 2H, <sup>3</sup>J = 3.7 Hz), 7.03 (dd, 2H, <sup>3</sup>J = 5.0 Hz, <sup>3</sup>J = 3.7 Hz), 6.95 (s, 2H), 6.93 (d, 2H, <sup>3</sup>J = 3.7 Hz); HRMS (EI) for C<sub>18</sub>H<sub>12</sub>S<sub>4</sub>, calcd 355.9821, obsd 355.9832.

**1,2-Bis[2-(5-hexyl-2-thienyl)-5-thienyl]ethene (H-T4V1b):** orange powder recrystallized from ethanol; yield 60%; mp 137 °C; <sup>1</sup>H NMR (CDCl<sub>3</sub>) δ 6.98 (d, 2H, <sup>3</sup>J = 3.8 Hz), 6.96 (d, 2H, <sup>3</sup>J = 3.8 Hz), 6.91 (s, 2H), 6.89 (d, 2H, <sup>3</sup>J = 3.7

Hz), 6.67 (d, 2H, <sup>3</sup>J = 3.7 Hz), 2.80 (t, 4H, <sup>3</sup>J = 7.5 Hz), 1.70 (m, 4H), 1.45–1.25 (m, 12 H), 0.92 (t, 6H, <sup>3</sup>J = 7.3 Hz); <sup>13</sup>C NMR (CDCl<sub>3</sub>) δ 145.7, 140.8, 136.8, 134.8, 126.9, 124.8, 123.4 (2C), 121.1, 31.6, 31.5, 30.2, 28.7, 22.5; HRMS (EI) for C<sub>30</sub>H<sub>36</sub>S<sub>4</sub>, calcd 524.1699, obsd 524.1694.

**General Procedure for the Wittig–Horner Olefination.** Under nitrogen atmosphere, potassium *tert*-butoxide was added portionwise to a mixture containing the aldehyde and the phosphonate in dry THF. The mixture was stirred at room temperature for 1 h. After evaporation of the solvent, the residue was taken with MeOH to give a precipitate. The solid was filtered then was washed twice with MeOH. The crude product was purified by recrystallization.

**(E,E)-5,5'-Bis[2-(2-thienyl)-1-ethenyl]thienylvinyl]-2,2'-bithiophene (H-T4V2a):** orange powder recrystallized from ethanol; yield 87%; mp 210 °C; <sup>1</sup>H NMR (C<sub>6</sub>D<sub>6</sub>) δ 6.99 (d, 2H, <sup>3</sup>J = 15.7 Hz), 6.93 (d, 2H, <sup>3</sup>J = 15.7 Hz), 6.86 (d, 2H, <sup>3</sup>J = 3.7 Hz), 6.73 (d, 2H, <sup>3</sup>J = 4.8 Hz), 6.68 (d, 2H, <sup>3</sup>J = 3.2 Hz), 6.65 (dd, 2H, <sup>3</sup>J = 4.8 Hz, <sup>3</sup>J = 3.2 Hz), 6.50 (d, 2H, <sup>3</sup>J = 3.7 Hz); HRMS (EI) for C<sub>20</sub>H<sub>14</sub>S<sub>4</sub>, calcd 381.9978, obsd 381.9966.

**(E,E)-5,5'-Bis[2-(5-hexyl-2-thienyl)-1-ethenyl]-2,2'-bithiophene (H-T4V2b):** orange powder recrystallized from ethanol; yield 65%; mp 154 °C; <sup>1</sup>H NMR (C<sub>6</sub>D<sub>6</sub>) δ 7.07 (d, 2H, <sup>3</sup>J = 15.7 Hz), 7.00 (d, 2H, <sup>3</sup>J = 15.7 Hz), 6.93 (d, 2H, <sup>3</sup>J = 3.8 Hz), 6.69 (d, 2H, <sup>3</sup>J = 3.5 Hz), 6.58 (d, 2H, <sup>3</sup>J = 3.8 Hz), 6.54 (d, 2H, <sup>3</sup>J = 3.5 Hz), 2.62 (t, 4H, <sup>3</sup>J = 7.5 Hz), 1.62–1.57 (m, 4H), 1.29–1.21 (m, 12 H), 0.92 (t, 6H, <sup>3</sup>J = 7.3 Hz); <sup>13</sup>C NMR (CDCl<sub>3</sub>) δ 145.8, 141.8, 140.0, 135.8, 126.6, 126.3, 124.7, 124.1, 122.1, 121.0, 31.6, 31.5, 30.4, 28.7, 22.5, 14.0; MALDI-TOF for C<sub>32</sub>H<sub>38</sub>S<sub>4</sub>, calcd 550.18, obsd 550.16; HRMS (EI) for C<sub>32</sub>H<sub>38</sub>S<sub>4</sub>, calcd 550.1856, obsd 550.1867. Anal. (Calcd): C, 69.95 (69.77); H, 6.94 (6.95).

**(E,E)-5,5'-Bis[2-(2-thienyl)-1-ethenyl]thienylvinyl]-2,2':5,2''-terthiophene (H-T5V2a):** orange powder; yield 85%; mp 260 °C dec; HRMS (EI) for C<sub>24</sub>H<sub>16</sub>S<sub>5</sub>, calcd 463.9856, obsd 463.9865. Solubility was too low to perform spectroscopic analyses.

**(E,E)-5,5'-Bis[2-(5-hexyl-2-thienyl)-1-ethenyl]-2,2':5,2''-terthiophene (H-T5V2b):** orange powder recrystallized from CHCl<sub>3</sub>–hexane; yield 72%; mp 228 °C dec; <sup>1</sup>H NMR (C<sub>6</sub>D<sub>6</sub>) δ 7.03 (d, 2H, <sup>3</sup>J = 15.7 Hz), 6.95 (d, 2H, <sup>3</sup>J = 15.7 Hz), 6.86 (s, 2H), 6.88 (d, 2H, <sup>3</sup>J = 3.7 Hz), 6.65 (d, 2H, <sup>3</sup>J = 3.5 Hz), 6.52–6.49 (m, 4H), 2.57 (t, 4H, <sup>3</sup>J = 7.5 Hz), 1.61–1.52 (m, 4H), 1.24–1.19 (m, 12 H), 0.86 (t, 6H, <sup>3</sup>J = 7.0 Hz); MALDI-TOF for C<sub>36</sub>H<sub>40</sub>S<sub>5</sub>, calcd 632.17, obsd 632.21; HRMS (EI) for C<sub>36</sub>H<sub>40</sub>S<sub>5</sub>, calcd 632.1734, obsd 632.1716. Anal. (Calcd): C, 68.47 (68.30); H, 6.25 (6.37).

**(E,E)-2,5-Bis[2-(5-hexyl-2-thienyl)-1-ethenyl]thiophene (T3V2b):** orange powder recrystallized from ethanol; yield 70%; mp 82–83 °C; <sup>1</sup>H NMR (CDCl<sub>3</sub>) δ 6.93 (d, 2H, <sup>3</sup>J = 15.7 Hz), 6.86 (d, 2H, <sup>3</sup>J = 15.7 Hz), 6.85 (s, 2H), 6.83 (d, 2H, <sup>3</sup>J = 3.6 Hz), 6.65 (d, 2H, <sup>3</sup>J = 3.6 Hz), 2.78 (t, 4H, <sup>3</sup>J = 7.5 Hz), 1.70–1.65 (m, 4H), 1.34–1.30 (m, 12 H), 0.90 (t, 6H, <sup>3</sup>J = 7.3 Hz); <sup>13</sup>C NMR (CDCl<sub>3</sub>) δ 145.71, 141.30, 140.06, 126.59, 126.22, 124.71, 121.95, 120.27, 31.56, 31.47, 30.42, 28.74, 22.55, 14.06; HRMS (EI) for C<sub>28</sub>H<sub>36</sub>S<sub>3</sub>, calcd 468.1979, obsd 468.1996. Anal. (Calcd): C, 70.88 (71.74); H, 7.73 (7.74); S, 20.00 (20.52).

**(E,E,E)-1,2-Bis[5-[2-(5-hexyl-2-thienyl)-1-ethynyl]-2-thienyl]ethene (T4V3b):** red powder recrystallized from CHCl<sub>3</sub>–hexane; yield 60%; mp 146–147 °C; <sup>1</sup>H NMR (CDCl<sub>3</sub>) δ 6.95 (d, 2H, <sup>3</sup>J = 15.7 Hz), 6.92 (s, 2H), 6.89 (d, 2H, <sup>3</sup>J = 4.0 Hz), 6.87 (d, 2H, <sup>3</sup>J = 4.0 Hz), 6.86 (d, 2H, <sup>3</sup>J = 15.7 Hz), 6.84 (d, 2H, <sup>3</sup>J = 3.8 Hz), 6.65 (d, 2H, <sup>3</sup>J = 3.8 Hz), 2.78 (t, 4H, <sup>3</sup>J = 7.3 Hz), 1.70–1.65 (m, 4H), 1.35–1.29 (m, 12 H), 0.90 (t, 6H, <sup>3</sup>J = 6.4 Hz); <sup>13</sup>C NMR (CDCl<sub>3</sub>) δ 145.8, 141.8, 141.0, 140.0, 127.7, 127.2, 126.7, 126.4, 122.2, 121.4, 120.2, 31.5, 31.4, 30.4, 28.7, 22.5, 14.0; HRMS (EI) for C<sub>34</sub>H<sub>40</sub>S<sub>4</sub>, calcd 576.2013, obsd 576.2036. Anal. (Calcd): C, 69.95 (70.78); H, 6.94 (6.99); S, 21.81 (22.23).

**(E,E,E)-2,5-Bis[2-[5-(5-hexyl-2-thienyl)-2-thienyl]-1-ethenyl]thiophene (T5V4b):** red powder recrystallized from

(26) (a) Spangler, C. W.; McCoy, R. *Synth. Commun.* **1988**, *18*, 51. (b) Kofmehl, G.; Bohn, G. *Chem. Ber.* **1974**, *107*, 2791.

(27) Wei, Y.; Yang, Y.; Yeh, J.-M. *Chem. Mater.* **1996**, *8*, 2659.

(28) Benahmed-Gasmi, A.; Frère, P.; Elandaloussi, E. H.; Roncali, J.; Orduna, J.; Garin, J.; Jubault, M.; Riou, A.; Gorgues, A. *Chem. Mater.* **1996**, *8*, 2291.

CH<sub>2</sub>Cl<sub>2</sub>–hexane; yield 65%; mp 208–209 °C; <sup>1</sup>H NMR (C<sub>6</sub>D<sub>6</sub>)  $\delta$  7.10 (d, 2H, <sup>3</sup>J = 15.4 Hz), 7.00 (d, 2H, <sup>3</sup>J = 15.4 Hz), 6.98 (s, 4H), 6.67 (d, 2H, <sup>3</sup>J = 3.1 Hz), 6.57–6.54 (m, 6H), 6.50 (d, 2H, <sup>3</sup>J = 3.3 Hz), 2.57 (t, 4H, <sup>3</sup>J = 7.5 Hz), 1.60–1.50 (m, 4H), 1.36–1.30 (m, 12 H), 0.87 (t, 6H, <sup>3</sup>J = 7.2 Hz); <sup>13</sup>C NMR (CDCl<sub>3</sub>)  $\delta$  145.94, 142.02, 141.61, 141.00, 140.02, 127.42, 127.35, 126.76, 126.48, 124.81, 122.30, 121.72, 121.37, 120.19, 31.61, 31.51, 30.48, 28.79, 22.61, 14.31; HRMS (EI) for C<sub>40</sub>H<sub>44</sub>S<sub>5</sub>, calcd 684.2047, obsd 684.2071. Anal. (Calcd): C, 69.85 (70.12); H, 6.12 (6.47); S, 23.14 (23.40).

**(E,E)-1,4-Bis(2-thienyl)buta-1,3-diene (T2B1a).** **Route A.** From phosphonate **Pa** and 2-(3-oxo-1-propenyl)thiophene **8**, 85% yield. **Route B.** from phosphonate **Pc** and 2-carbaldehydethiophene **10**: 60% yield; yellow powder recrystallized from ethanol; mp 174 °C (lit.<sup>29</sup> mp 173 °C); <sup>1</sup>H NMR (C<sub>6</sub>D<sub>6</sub>)  $\delta$  6.74 (d, 2H, <sup>3</sup>J = 5.0 Hz), 6.71 (d, 2H, <sup>3</sup>J = 3.6 Hz), 6.68 (dd, 2H, <sup>3</sup>J = 5.0 Hz, <sup>3</sup>J = 3.6 Hz), 6.60 (2H, AA' part of the AA'XX' system, J<sub>AX</sub> = 15.3 Hz, J<sub>AA'</sub> = 10.3 Hz, J<sub>AX'</sub> = 0.5 Hz, J<sub>XX'</sub> = 0 Hz), 6.35 (2H, XX' part of the AA'XX' system', J<sub>AX</sub> = 15.3 Hz, J<sub>AA'</sub> = 10.3 Hz, J<sub>AX'</sub> = 0.5 Hz, J<sub>XX'</sub> = 0 Hz).

**(E,E,E,E)-2,5-Bis[4-(2-thienyl)-1,3-butadienyl]thiophene (T3B2a):** yellow powder recrystallized from CHCl<sub>3</sub>–hexane; yield 74%; mp 212 °C (lit.<sup>7</sup> mp 212 °C); <sup>1</sup>H NMR (C<sub>6</sub>D<sub>6</sub>; see text and Table 1 for the discussion)  $\delta$  6.78 (d, 2H, <sup>3</sup>J = 5.0 Hz), 6.72 (d, 2H, <sup>3</sup>J = 3.5 Hz), 6.68 (dd, 2H, <sup>3</sup>J = 5.0 Hz, <sup>3</sup>J = 3.5 Hz), 6.65 (AA', 4H), 6.62 (s, 2H), 6.41 (XX', 2H), 6.32 (XX', 2H); <sup>13</sup>C NMR (CDCl<sub>3</sub>)  $\delta$  142.89, 142.02, 128.73, 128.51, 127.72, 127.16, 126.02, 125.61, 125.46, 124.56; HRMS (EI) for C<sub>20</sub>H<sub>16</sub>S<sub>3</sub>, calcd 352.0414, obsd 352.0420. Anal. (Calcd): C, 67.74 (68.14); H, 4.80 (4.57).

**(E,E,E,E,E)-1,4-Bis[5-[1-(4-(2-thienyl))-1,3-butadienyl]-2-thienyl]buta-1,3-diene (T4B3a):** orange powder; yield 60%; HRMS (EI) for C<sub>28</sub>H<sub>22</sub>S<sub>4</sub>, calcd 486.0604, obsd 486.0601. Solubility was too low to perform spectroscopic analyses.

**(E,E,E,E)-2,5-Bis[1-[4-(5-hexyl-2-thienyl)]-1,3-butadienyl]thiophene (T3B2b):** orange powder recrystallized from CHCl<sub>3</sub>–hexane; yield 66%; mp 119–120 °C; <sup>1</sup>H NMR (C<sub>6</sub>D<sub>6</sub>; see text and Table 1 for the discussion)  $\delta$  6.74–6.62 (m, 6H), 6.60 (s, 2H), 6.53 (d, 2H, <sup>3</sup>J = 3.7 Hz), 6.45 (XX', 2H), 6.35 (XX', 2H), 2.75 (t, 4H, <sup>3</sup>J = 7.5 Hz), 1.70–1.60 (m, 4H), 1.33

(m, 12 H), 0.87 (t, 6H, <sup>3</sup>J = 7.2 Hz); <sup>13</sup>C NMR (CDCl<sub>3</sub>)  $\delta$  145.87, 141.99, 140.53, 128.91, 127.31, 126.87, 126.17, 126.09, 125.60, 124.76, 31.48, 30.42, 29.69, 28.74, 22.60, 14.08; HRMS (EI) for C<sub>32</sub>H<sub>40</sub>S<sub>3</sub>, calcd 520.2292, obsd 520.2290. Anal. (Calcd): C, 74.03 (73.79); H, 7.68 (7.74); S, 18.71 (18.47).

**(E,E,E,E,E)-1,4-Bis[5-[4-(5-hexyl-2-thienyl)-1,3-butadienyl]-2-thienyl]buta-1,3-diene (T4B3b):** red powder recrystallized from CHCl<sub>3</sub>; yield 70%; mp 195 °C dec; <sup>1</sup>H NMR (CDCl<sub>3</sub>)  $\delta$  6.85 (d 2H, <sup>3</sup>J = 3.8 Hz), 6.83 (d 2H, <sup>3</sup>J = 3.8 Hz), 6.80 (d 2H, <sup>3</sup>J = 3.5 Hz), 6.74–6.54 (m, 14H), 2.8 (t, 4H, <sup>3</sup>J = 7.5 Hz), 1.60–1.50 (m, 4H), 1.30–1.10 (m, 12 H), 0.87 (t, 6H, <sup>3</sup>J = 7.2 Hz); <sup>13</sup>C NMR (CDCl<sub>3</sub>)  $\delta$  145.94, 142.35, 141.85, 140.85, 131.12, 129.03, 128.65, 127.27, 126.93, 126.22, 125.59, 124.77, 124.70, 31.55, 30.42, 28.74, 22.56, 17.14, 14.07, 13.08; HRMS (EI) for C<sub>40</sub>H<sub>46</sub>S<sub>4</sub>, calcd 654.2482, obsd 654.2478. Anal. (Calcd): C, 73.18 (73.34); H, 7.10 (7.08).

**X-ray Crystallography of 14.** Single crystals were mounted on an Enraf-Nonius MACH3 diffractometer with graphite monochromator and Mo K $\alpha$  ( $\lambda$  = 0.717 03 Å) radiation at T = 294 K. The data collections were performed with the  $\omega/2\theta$  scan technique. The crystal structures were solved by direct method (SIR) and refined by full matrix least squares techniques using ShelX software. The positions of hydrogen atoms were obtained from Fourier difference.

Crystal data of **14**: C<sub>18</sub>H<sub>14</sub>S<sub>2</sub>O<sub>2</sub>, triclinic space group *P*-1, *a* = 3.929(2) Å, *b* = 10.03(1) Å, *c* = 11.00(1) Å,  $\alpha$  = 114.3(1)°,  $\beta$  = 92.98(8)°,  $\gamma$  = 92.90(7)°, *V* = 393(1) Å<sup>3</sup>, *Z* = 1, *T* = 293 K, *F*(000) = 170,  $\mu$ (Mo K $\alpha$ ) = 0.341 mm<sup>-1</sup>; 1458 reflections collected from which 1381 (*R*<sub>int</sub> = 0.032) were independent, 1032 reflections with *I* > 2 $\sigma$ (*I*), 128 refined parameters, *R*<sub>1</sub> = 0.045, *wR*<sub>2</sub> (all data) = 0.114.

**Acknowledgment.** Financial support from MCyT-FEDER (Project No. BQU2002-00219) and Gobierno de Aragón-Fondo Social Europeo (Project No. P-009-2001) is gratefully acknowledged.

**Supporting Information Available:** The X-ray data of **14** in CIF format. This material is available free of charge via the Internet at <http://pubs.acs.org>.

(29) Ribereau, P.; Pastour, P. *Bull. Soc. Chim. Fr.* **1969**, *6*, 2076.